Nano Research

ISSN 1998-0124 CN 11-5974/O4
https://doi.org/10.1007/s12274-023-5804-x

Research Article

# Piezoelectric wearable atrial fibrillation prediction wristband enabled by machine learning and hydrogel affinity

Yuan Xi[1], Sijing Cheng[3], Shengyu Chao[2], Yiran Hu[3], Minsi Cai[3], Yang Zou[4], Zhuo Liu[1], Wei Hua[3] (✉), Puchuan Tan[2] (✉), Yubo Fan[1] (✉), and Zhou Li[2,5,6,7] (✉)

[1] *Beijing Advanced Innovation Centre for Biomedical Engineering, Key Laboratory for Biomechanics and Mechanobiology of Ministry of Education, School of Biological Science and Medical Engineering, School of Engineering Medicine, Beihang University, Beijing 100191, China*
[2] *CAS Center for Excellence in Nanoscience, Beijing Key Laboratory of Micro-nano Energy and Sensor Beijing Institute of Nanoenergy and Nanosystems, Chinese Academy of Sciences, Beijing 101400, China*
[3] *The Cardiac Arrhythmia Center, State Key Laboratory of Cardiovascular Disease, National Clinical Research Center of Cardiovascular Diseases, Fuwai Hospital, National Center for Cardiovascular Diseases, Chinese Academy of Medical Sciences and Peking Union Medical College, Beijing 100037, China*
[4] *School of Life Science, Institute of Engineering Medicine, Beijing Institute of Technology, Beijing 100081, China*
[5] *School of Nanoscience and Technology, University of Chinese Academy of Sciences, Beijing 100049, China*
[6] *Center on Nanoenergy Research, School of Physical Science and Technology, Guangxi University, Nanning 530004, China*
[7] *Institute for Stem Cell and Regeneration, Chinese Academy of Sciences, Beijing 100101, China*



**Received:** 1 February 2023 / **Revised:** 7 April 2023 / **Accepted:** 3 May 2023

## ABSTRACT

Atrial fibrillation (AF) is a common and serious disease. Its diagnosis usually requires 12-lead electrocardiogram, which is heavy and inconvenient. At the same time, the venue for diagnosis is also limited to the hospital. With the development of the concept of intelligent medical, a wearable, portable, and reliable diagnostic method is needed to improve the patient's comfort and alleviate the patient's pain. Here, we reported a wearable atrial fibrillation prediction wristband (AFPW) which can provide long-term monitoring and AF diagnosis. AFPW uses polyvinylidene fluoride piezoelectric film as sensing material and hydrogel as skin bonding material, of which the structure and design have been optimized and improved. The hydrogel skin bonding layer has good stability and skin affinity, which can greatly improve the user experience. AFPW has enhanced signal, strong signal-to-noise ratio, and wireless transmission function. After a sample library of 385 normal people/patients is analyzed and tested by linear discriminant analysis, the diagnostic success rate of atrial fibrillation is 91%. All these excellent performances demonstrate the great application potential of AFPW in wearable device diagnosis and intelligent medical treatment.

## KEYWORDS

piezoelectricity, atrial fibrillation prediction, machine learning, wristband

## 1 Introduction

Atrial fibrillation (AF) is a common arrhythmia in clinic, whose incidence rate and prevalence rate are on the rise in recent years [1, 2]. Epidemiological investigation of atrial fibrillation shows that the incidence rate among residents over 80 years old is 10% and the prevalence rate of atrial fibrillation in China is 0.71% [3, 4]. Moreover, more and more patients may lead to a variety of complications, including cerebral apoplexy, heart failure, and dementia, with high modality and disability rates [5, 6]. Due to the extensive and serious harm of AF, the accurate diagnosis of AF is particularly important [7]. The clearest diagnosis of AF is 12-lead electrocardiogram (ECG). However, research shows that traditional ECGs are very likely to miss cases, for paroxysmal atrial fibrillation (PAF) is not always detectable [8]. Traditional 12-lead ECG is too heavy and inconvenient for persistent monitoring. Thus, wearable devices are developed to detect AF, such as Holter monitors, single-lead electrocardiogram, photoplethysmography (PPG), etc. [9]. Nonetheless, these devices do not meet the requirements of diagnosis perfectly. Holter monitors still offer limited duration of continuous monitoring, and Holter monitors are not completely comfortable for patients [10]. Single-lead electrocardiogram shows its limitations when analyzing more complex rhythms. PPG decreases in analysis accuracy when working on different skin tones, skin moisture levels, and tattoos [11].

Radial pulse wave is an important physiological detection signal, which is widely used in wearable devices [12]. Traditional medical diagnosis, especially in China, regards radial artery pulse as most conclusive part of diagnosis [13, 14]. Traditional pulse diagnosis requires extensive experience, which may not be judged accurately due to doctors' subjective consciousness. Nowadays, precise measurement of pulse wave becomes possible using different types of sensors [15]. The further effective analysis of pulse wave signal makes it an important physiological signal in

Address correspondence to Wei Hua, drhua@vip.sina.com; Puchuan Tan, tanpuchuan@binn.cas.cn; Yubo Fan, yubofan@buaa.edu.cn; Zhou Li, zli@binn.cas.cn

modern medicine. Pulse wave has the same excitation source as ECG, which shows abnormal pulse wave when AF occurs, due to insufficient blood ejection and irregular frequency [16]. Scientific processing of collected pulse wave signals can effectively diagnose AF.

Machine learning, as the core of artificial intelligence (AI), has been used in medical diagnosis research. Through the method of data processing and machine learning, the AF signals are possibly to be identified without experienced doctors [17]. Selected features are extracted to import into machine learning model for recognition. Unlike traditional data analysis methods, AI-assisted diagnosis only requires presence of an experienced doctor when building and training a computer model, but no longer when using model, which means significant savings in medical and human resources [18]. What's more, the AI-assisted diagnosis will not be as tiring as human, and results can be obtained in a short time. While AI-assisted diagnosis cannot be used as the gold standard to identify diseases, it can still be used as a recognition tool with high accuracy [19].

Piezoelectric nanogenerator (PENG) is an excellent sensor functional module because of its ability to transform small mechanical signal into electrical signal through piezoelectric effect, and shows potential application prospects in self powered systems, wearable electronics, and sensory devices [20]. Unlike inorganic piezoelectric material, polyvinylidene fluoride (PVDF) is flexible and ductile, making it popular when designing wearable sensors [20–23]. Moreover, PVDF preparation process is simple, the cost is low, and the durability is excellent [24–27]. In order to make PVDF fit the human skin better, the auxiliary materials with better adhesion and fit are also considered. Hydrogels are widely used in wearable sensors because of good biocompatibility, degradability, renewable, and other characteristics [28, 29]. Hydrogels are usually composed of hydrophilic polymer networks. These polymers make the hydrogel surface contain a large number of –OH, –COOH, and $-NH_2$ groups, which enable the hydrogel to be well adsorbed on skin, glass, rubber, metal, and other surfaces [30]. The stability of hydrogel is poor, and it is difficult to maintain excellent performance in dry or low-temperature environment [31]. To solve these defects, the method of adding inorganic salt or using organic solvent aqueous biphase system in the preparation process of hydrogels is usually selected, so that hydrogels can be stable in dry environments by improving their water retention performance [32, 33].

Here, we reported a wearable atrial fibrillation prediction wristband (AFPW) which can provide long-term monitoring and AF diagnosis. AFPW consists of sensing part and supporting part. The sensing part is based on piezoelectric effect and thus is self-powered. Moreover, the mechanical and electrical performances of sensing parts with different structure designs were measured and compared. It can receive pulse wave signals up to 1.4 V and the signal-to-noise ratio (SNR) is 37 dB. Furthermore, an AF prediction AI model was built after machine learning a sample library of 385 normal people/patients, and 91% diagnostic accuracy is obtained, which illustrates excellent potential for medical treatment and comfortable medical treatment.

## 2 Results and discussion

### 2.1 Material and structure

Figure 1(a) presents schematic illustration of AFPW, which consists of sensor part and supporting part. Sensor part realizes the function of collecting pulse wave signals, which contains PVDF piezoelectric film, polytetrafluoroethylene (PTFE) encapsulation layer, enhancement layer, and hydrogel adhesive layer. PVDF uses piezoelectric effect to convert pulse wave signal into electrical signal, which is the functional layer of the AFPW. PTFE encapsulation layer protects both sensors and skin, which can maintain the sensor function for a long time and improve the comfort of users. What's more, PTFE encapsulation layer can specifically enhance pulse wave signal though shows average performance in other signals. Young's modulus of PTFE encapsulation layer is close to skin, and it is speculated that the high matching degree of Young's modulus may enhance the signal. The enhancement layer is three-dimensional (3D) printed and consists of a series of micro-pillars with a spacing of 1 mm and a height of 2 mm. The comparison of pulse wave output with or without enhancement layer is shown in Fig. S1 in the Electronic Supplementary Material (ESM). As can be seen, the output with an enhancement layer added greatly exceeds the output without an enhancement layer. This proves the important role of the enhancement layer for output enhancement. The enhancement layer with designed structure is placed on the back side of PVDF to enhance signal. The hydrogel surrounds the whole system making the device fit better and more comfortable with the skin. Supporting part consists of Bluetooth module, polylactic acid (PLA) shell, and rubber base. Bluetooth module, which made up of Bluetooth and battery, transmits signal to computer or cell phone for further analysis. Bluetooth module used in this work is HC-05. PLA shell protects and supports Bluetooth module within it and sensors below it, which is 3D printed. Rubber base constitutes the main physical support structure of the bracelet. Figure 1(b) shows the information transmission of AFPW. The mechanical signal of pulse wave is converted into electrical signal and transmitted to the processing terminal. After machine learning analysis, the judgments and expectations of probability of illness are sent to medical staff for further treatment. As shown in Figs. 1(c)–1(f), AFPW is as large as a watch while the sensor part can fit human skin well.

Linear discriminant analysis (LDA) is chosen as machine learning analysis algorithm in this article. LDA is a classical linear learning method which uses statistics and pattern recognition methods to try to find a linear combination of the characteristics of many types of objects or events, so that they can be characterized or distinguished. In this work, the total sample size is 385. Features engineering is determined by the characteristics of pulse wave signal and pathological information analyzed. Important parameters of signals are selected as features such as average value and peak value. The accuracy of patient identification is high (91%), and the clustering and distinguishing are good (Fig. 1(g)). It is noteworthy that the undetected rate of patients is only 1%, which means diagnosing AF promptly and treating patients without delay. The complete diagnostic system is presented in Fig. 1(h), which is established on AFPW. The sensor part collects and transfers information of pulse wave, converting mechanical signal to electrical signal. The analysis system receives and processes data, then extracts features for LDA model, which gives an automatic diagnosis of AF. The diagnosis and data will be an import basis and criteria for doctors and patients. It is helpful for early diagnosis and timely treatment of AF.

Figure 2(a) shows the structure of sensor part and how AFPW works on the vessel and skin. The beat with pulse is transmitted from blood vessel through skin to the sensor. The encapsulation layers of PTFE amplify the pulse wave signal by appropriate elastic property, while the enhancement layer also enhances the signal by hard base. The functional layer includes PVDF piezoelectric film and silver electrodes on it, which generate piezoelectric signal for further analysis. The operating principle of AFPW is shown in Fig. 2(b). At the initial state, the whole system is in resting rate, and there is no current flowing through external circuit. When the

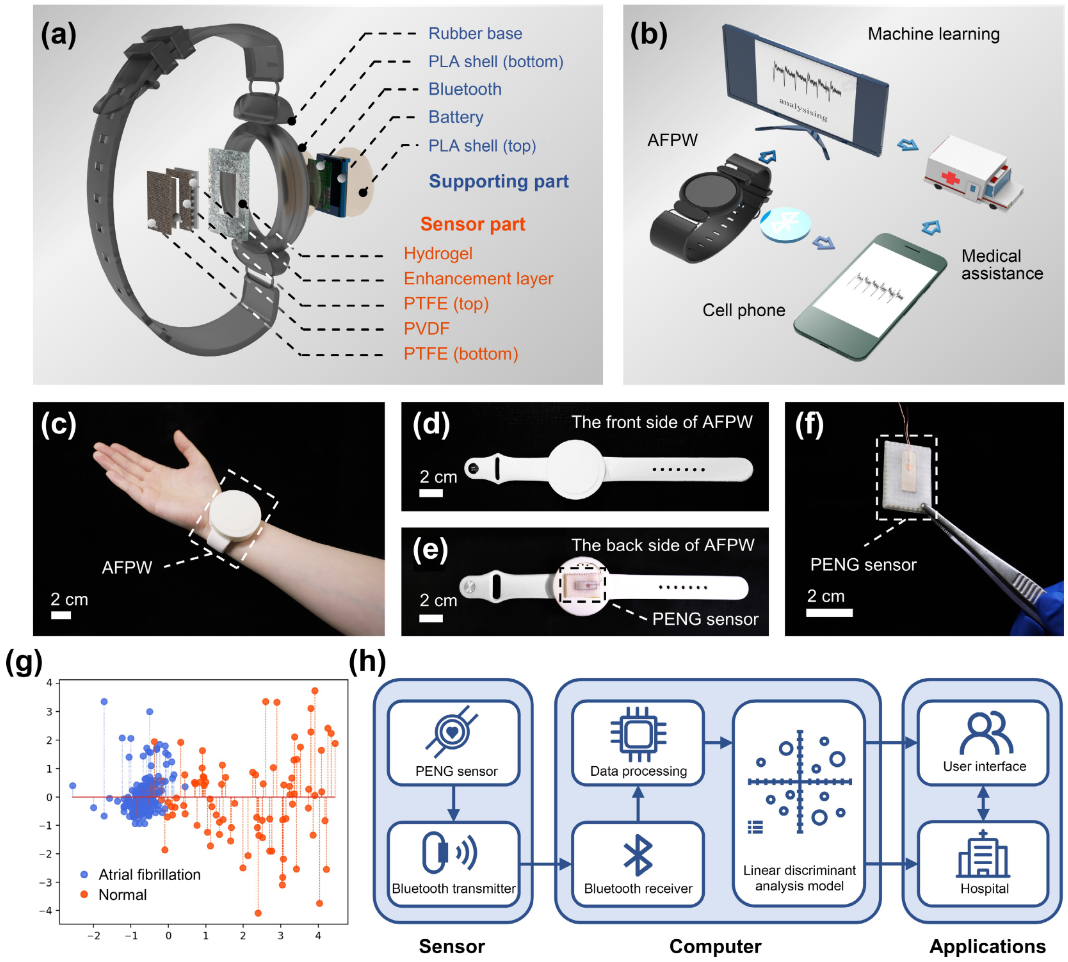


**Figure 1** Overview of AFPW. (a) Schematic diagram of sensor part and supporting part of AFPW. (b) Information transmission of AFPW. (c)–(f) Photographs of AFPW. (g) LDA cluster distribution. (h) The design concept of AFPW.

pulse starts to beat, the deformation of PVDF piezoelectric film generates the induced charge due to the piezoelectric effect. Between silver electrodes appears potential difference, and the current flows in the external circuit, which can be monitored and analyzed. When pulse beat reaches the peak value, the voltage extreme value generated by induced charge reaches the maximum. After the extreme value, the whole system reverts to the original state and causes a reverse flow of current in the external circuit. This process will continue until the resting state is restored. The COMSOL simulations of piezoelectric effect and deformation are shown in Figs. 2(c) and 2(d). It can be found that a discernible signal is generated in a minor deformation. This proves that the tiny pulse wave beating can produce obvious piezoelectric effect and can be accurately identified and analyzed. In simulation, the electronic components are shown in Fig. 2(e). PENG sensor is the key part of the whole system, which collects pulse wave signal. Bluetooth transmitter and battery constitute transmitting part, which can transmit signal to receiver for further analysis. Bluetooth receiver and Arduino circuit board receive signal from transmitting part and present it to signal processor. Bluetooth transmitter and battery are inside the AFPW, while Bluetooth receiver and Arduino circuit board are connected to the computer. Figure 2(f) presents circuit diagram and how circuit realizes functions. Pulse wave signal is collected by sensor, transmitted through Bluetooth, and pre-signal processed by Arduino Uno. Figure 2(g) presents the relationship diagram of the force and electrical signals simulated by COMSOL. Figure 2(g) presents positive correlation with good linearity between the force–electricity relationship within a certain range, which demonstrates the sensor's good ability to transform and transmit pulse wave information effectively and accurately. Figures 2(h)–2(j) show the open-circuit voltage ($V_{OC}$), short-circuit current, and charge transfer amount when AFPW is monitoring pulse wave signal directly, which showed the characteristics of electrical signals. The peak voltage output is 0.75 V, the peak current output is 0.45 μA, and the single charge transfer amount is 28 nC, respectively.

### 2.2 Characterization and optimization

To enhance signal output and signal-to-noise ratio, multiple parameters and structures of AFPW were measured and designed. PVDF encapsulation layer tremendously affected the output of AFPW (shown in Fig. 3(a)). When the thickness of front side is 0.24 mm and the thickness of back side is 0.24 mm, the highest output is reached, which are the best parameters for pulse wave detection. As shown in Fig. 3(b), to explore the optimal aspect ratio of PVDF under the same area conditions, different aspect ratios along the direction of blood flow (shown as *a*/*b*) were tested, and the results show that 3:1 is the best aspect ratio under fixed PVDF area. Figure 3(c) shows that PVDF thickness affects output and thicker performs better, but too thick PVDF will hinder encapsulation and destroy comforts of users, so the thickness of 110 μm is chosen. Figure 3(d) shows a rapid applied stress cycle. In this cycle, the response time is 0.027 s, which is short enough to reflect real-time details. Besides, the well match of the applied force and the $V_{OC}$ response has been verified, and its real-time and quick response ability plays an important role in signal acquisition and processing. Figure 3(e) presents good linear relationship between force and $V_{OC}$, with a coefficient of determination of 0.98218, which means AFPW can collect force signals linearly and

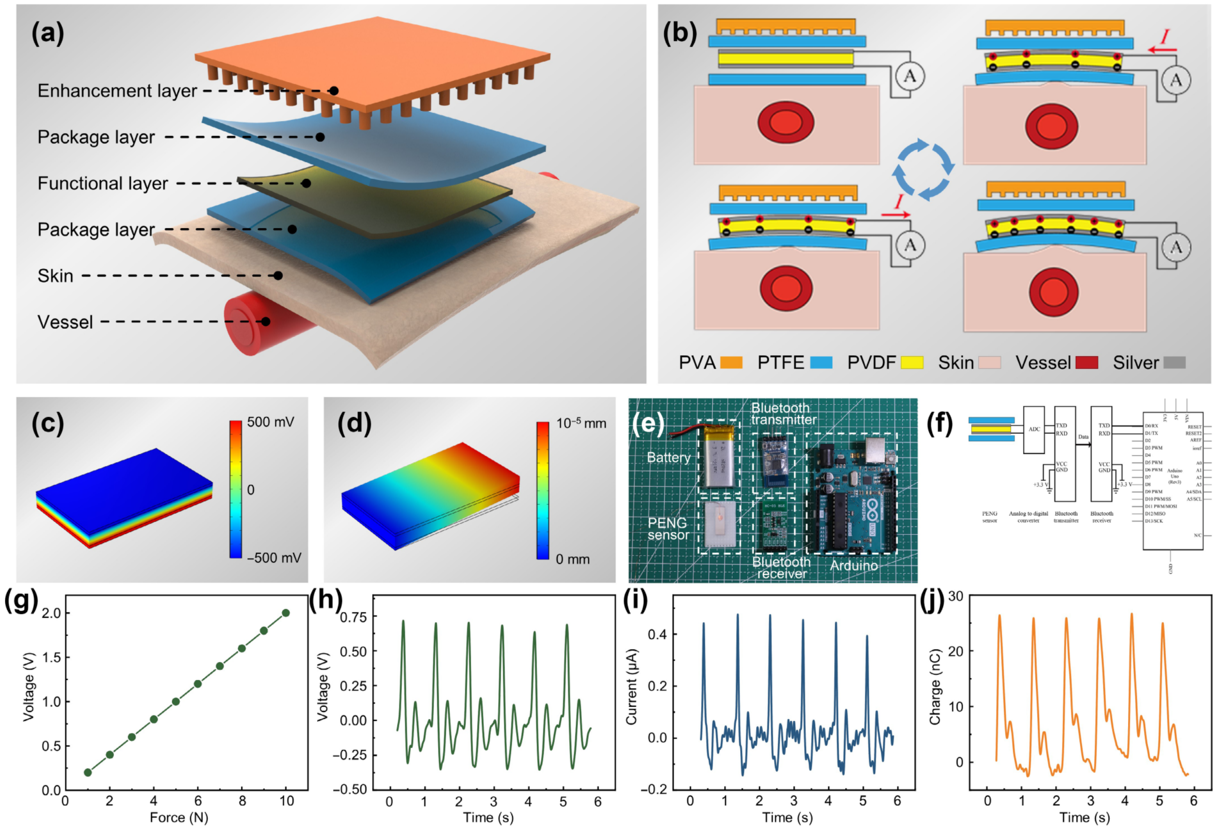


**Figure 2** Operating principle of AFPW. (a) The structure and materials used of sensor in AFPW. (b) The electric generation principle of AFPW. (c), (d), and (g) COMSOL simulations of AFPW. (e) Circuit elements used by AFPW. (f) The circuit diagram of the AFPW. (h) The open-circuit voltage of AFPW. (i) The short-circuit current of AFPW. (j) Amount of transferred charge.

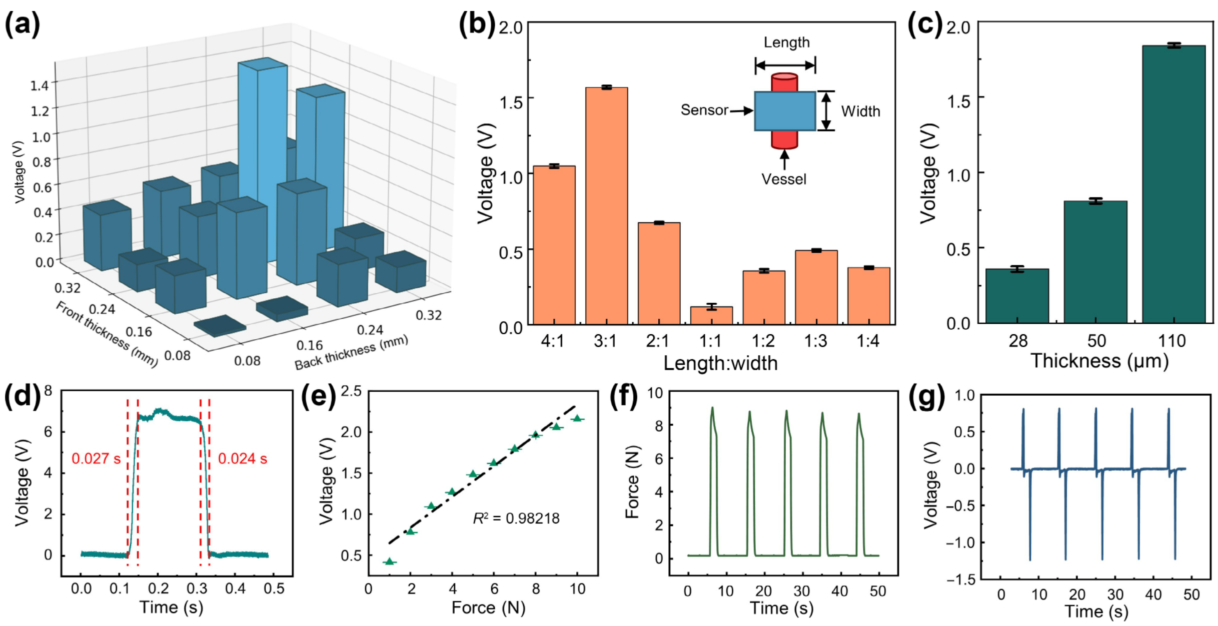


**Figure 3** Output improvement due to different designs and parameters. (a) Influence of different thicknesses of encapsulation layer on output. (b) Influence of different aspect ratios on output. (c) Influence of different thicknesses of PVDF piezoelectric film. (d) Response time of AFPW. (e) Relationship between force and electricity. (f) and (g) Force and electricity performances of AFPW.

convert them into electrical signals within a certain range. Figure S2 in the ESM explores the output variation under the action of a smaller range of forces, and it can be seen that the output also exhibits good linearity. When periodic forces are applied to AFPW (Fig. 3(f)), electrical signals with high repeatability are collected (Fig. 3(g)), and the result obtained by repeated times is recorded with error calculated. The signal shown in Fig. 3(g) is triggered by a force of the magnitude shown in Fig. 3(f). Figure 4(a) shows the signal-to-noise ratio of AFPW, which is 37 dB. Good signal-to-noise ratio can reduce interference and improve signal quality. As shown in Table S1 in the ESM, AFPW shows good signal-to-noise ratio performance in similar researchs.

In order to enhance comfort and fit with skin, the hydrogel layer was used on the surface of AFPW in contact with the skin. Hydrogel has great advantages in mechanical properties, water permeability, air permeability, moisture retention, biological activity, biocompatibility, etc. Herein hydrogel, as skin affinity adhesive material, closely fits with skin to enhance signal

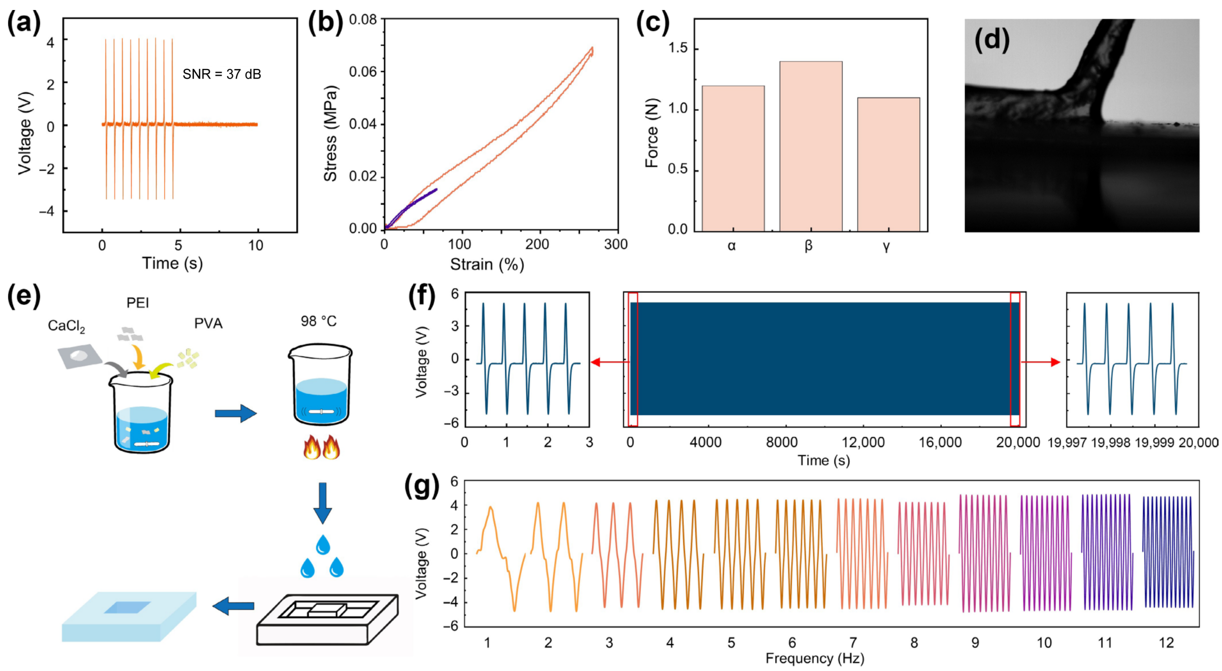


**Figure 4** Hydrogel performance and stability of AFPW. (a) Signal-to-noise ratio of AFPW. (b) Stress–strain curves of hydrogel under different loads. (c) Adhesion properties of different hydrogels. (d) Adhesion effect of hydrogel photographed by contact angle measuring instrument. (e) Schematic diagram of fabrication process of hydrogel. (f) Cyclic stability of AFPW. (g) Influence of frequency on output.

reception. Figure 4(b) shows strain–stress curves of hydrogel, which represent its mechanical properties in deformation and reverse deformation. When hydrogel slides, translates, and twists with the skin due to human motion, excellent mechanical properties ensure that the hydrogel will not be damaged and maintain its function. At lower strains, the loading and unloading curves basically coincide. Under high strain, the curve exhibits significant hysteresis loops, but the residual strain is only 40%. This shows that the effluent gel has good mechanical recovery performance. Figure 4(c) shows how different preparation methods affect adhesion property. Different masses of $CaCl_2$ (3.5, 4, and 4.5 g compared with standard production process as mentioned below are applied to α, β, and γ) in hydrogel production process created hydrogels with slightly different properties. Figure 4(c) shows how much force needs to be used to lift the hydrogel from the skin. Figure 4(d) is filmed with contact angle meter, which shows the moment of hydrogel pulling up from the skin. Certain adhesion can be observed between skin and hydrogel. Adhesiveness is strong to fit skin, and is not too strong to injure skin. Figure 4(e) presents the preparation process of hydrogel. 2 g poly(vinyl alcohol) (PVA), 1 g poly(ethylene imine), and 4 g $CaCl_2$ were mixed in 9 mL of deionized water. Then, the mixture was heated in a water bath of 98 °C for 2 h, and the product was poured into the mold and freezed for 12 h to get the hydrogel. Figure 4(f) shows the stability of AFPW. After 20,000 periodic tests, the output of AFPW remains almost unchanged, which shows great stability. Under normal circumstance, the beating rate of the atrium is approximately 60 to 100 beats per minute. In cases of atrial fibrillation, the beating rate of the atrium may be very fast, reaching 400–600 beats per minute. Figure 4(g) shows output of AFPW in different frequencies covering the heart rates of normal people and patients. Their outputs are relatively consistent in the whole heart rate ranges, which shows good stability in frequency. In order to verify that the device output is a piezoelectric signal rather than a triboelectric electrical signal, nylon was used instead of PVDF for testing, as shown in Fig. S3 in the ESM. It can be seen that no obvious signal appeared, indicating that the output of AFPW is a piezoelectric signal rather than a triboelectric electrical signal.

### 2.3 Signal processing and model establishment

The use of pulse wave signal mainly has the following difficulties [15, 34]: (1) The signal frequency is low. Pulse wave signal frequency is low and difficult to identify. (2) The signal is weak and vulnerable to interference. (3) Signals are variable. Different people under the same conditions, or the same person at different times, will show different pulse wave waveforms, which is a difficult problem in the analysis. (4) The amount of signal data is large. The pulse wave signal collected in clinic needs to be recorded for a long time. In order to record more information, the sampling rate will also be increased, and the amount of data will be further increased. Problems of frequency and signal stability are solved by precision AFPW sensor. Signal variability needs to be solved by long-term signal monitoring, which can be solved by the portable and wearable sensor of AFPW. However, long-term signal monitoring increases data volume and aggravates the difficulty of manual data analysis. In view of the large amount of signal data, it is necessary to introduce the computer-aided judgment method to deal with the huge amount of data that cannot be processed by humans.

Data analysis is an important method to judge the condition of the disease. Usually, this process is completed by doctors, but the number of doctors is insufficient and the accuracy is limited by the experience of doctors. Therefore, the data analysis method of machine learning is introduced. Figures 5(a) and 5(b) show pulse waves of normal people and patients with AF, respectively. As can be seen, pulse waves of normal people are stable and regular, and pulse waves of patients with atrial fibrillation are disordered and irregular. The waveform of pulse wave mainly consists of two parts, which are progressive wave and reflected wave. The heart emits blood regularly and intermittently, and transmits the pulse wave from the aortic root along the arterial system. The periodic ejection of the heart leads to the regular pulsation of the blood pressure and the regular pulsation of the arterial wall. The rhythm of the arterial system will directly affect the downstream adjacent segment, making it also follow the periodic pulsation. As shown in Fig. 5(c), this wave is called the progressive wave. In the process of transmission, there is a reflection phenomenon of human pulse

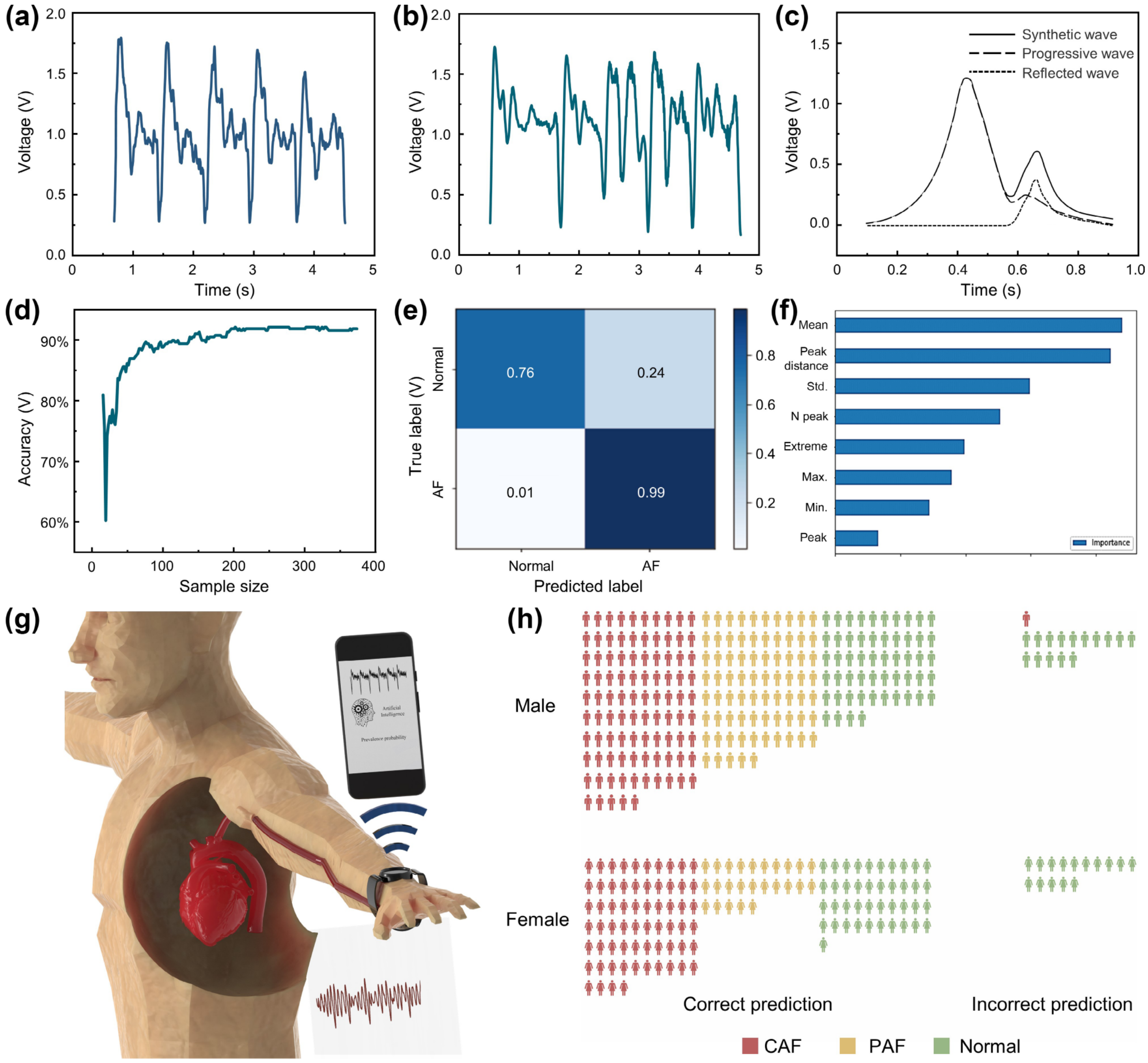


**Figure 5** Processing methods and results of machine learning. (a) Pulse wave of normal people. (b) Pulse wave of patients with AF. (c) The formation principle of pulse wave. (d) Prediction accuracy of model as sample size increases. (e) Confusion matrix of machine learning. (f) Feature importance in machine learning. (g) Information transmission process of the system. (h) Patient information and the numbers of correct prediction and incorrect prediction.

wave. These waves are caused by the collision and reflection of blood and blood vessels. Because the heart beat drives blood circulation, pulse wave contains various information about normal beat and abnormal beat, which can be recognized by signal processing. From the perspective of hemodynamics, the pressure wave of the radial artery is actually transmitted into the brachial artery and reaches the radial artery when the heart contracts and ejects blood. The pathological changes of some blood vessels or tissues and organs will lead to changes in the regularity of pulse waves, which will affect the characteristics of pulse waves. The pulse of atrial fibrillation will have obvious irregular beats. In typical patients with atrial fibrillation, the pulse rate is less than the heart rate. Because atrial fibrillation does not maintain enough blood volume of peripheral arterial pulsation, every time the heart contracts, the pulse of atrial fibrillation is uneven. The proof of the pulse wave and the formation mechanism prove that the pulse wave contains sufficient information of cardiac disease, which shows that AF can be analysed and diagnosed through pulse wave.

Here, LDA is used for data analysis and discrimination. LDA is a dimension reduction technology of supervised learning, which means that each sample of its dataset has category output. The basic idea of LDA is: Given the training sample set, try to project the sample onto a straight line, so that the projection point of the same sample is as close as possible, and the projection point center of the different samples is as far away as possible. The feature extraction of the sample is based on the characteristics of pulse wave and the pathological characteristics of AF, and multiple characteristic values are designed for comparison. The final selected features include average, peak-to-peak, maximum, minimum, etc. As shown in Fig. 5(d), with the increase of sample size, the accuracy has been greatly improved. In the analysis with sample size more than 200, the accuracy rate will not change significantly, indicating that the experimental sample is sufficient for LDA analysis. Shown as Fig. 5(e), in the overall data analysis, the error mainly occurs in the false detection of normal patients, which can be excluded by re-examination, and almost all the cases of AF are found, which is extremely important in large-scale physical examination. The overall recognition accuracy is up to 91%. Among the many features screened, the most effective features are listed in Fig. 5(f), of which the average and peak contribute the most to the analysis process. Figure 5(g) shows the information transmission process of the system. The heart pulsation supplies blood to the whole body and carries pulsation information. The pulse wave signal is received by AFPW at the wrist, transmitted to the processing terminal through Bluetooth, and then processed and analyzed at the terminal, and the disease risk is obtained. Figure 5(h) shows the patient information and the number of successful identifications. It can be seen that the recognition success rates of male and female patients are both high, the errors are mainly concentrated in the false detection part, and the number of missed inspections is small.

### 2.4 Materials and methods

Molds for the atrial fibrillation prediction wristband were designed and printed using a three-dimensional printer (Raize 3D) and PLA printing supplies. PVDF was manufactured by VKINGING Co., Ltd. For wireless data acquisition and transmission, a commercial Bluetooth board and Arduino Uno were used. A linear motor (LinMot E1100, Suzhou, China) was utilized to continuously impart periodic mechanical traction to the AFPW to maintain the operating cycle. A Keithley 6517 electrometer (Beijing, China) was used to measure the electrical signal of the AFPW, and the data were obtained and recorded using an oscilloscope (LeCroy HDO6104, New York, NY, USA). A wireless motion monitoring system based on a BMD101 board was used to record data from the AFPW. An ESM301/Mark-10 system was used for the cyclic press–release test, and a Mark-10 force gauge was used to detect the applied force and corresponding displacement under compression.

## 3 Conclusions

In summary, we reported a wearable and wireless piezoelectric disease monitoring bracelet (AFPW), which can automatically analyze the wearer's pulse wave signal and calculate the wearer's risk of developing atrial fibrillation, with an accuracy of 91%. Different structures of AFPW have been fabricated, compared, and optimized to enhance the sensor output. In order to enhance the fit between the sensor and the skin and receive the signal better, a hydrogel bonding layer was added and improved. The improvement of material and structure increases the output and stability of the sensor. Through linear discriminant analysis of a large amount of data, AFPW can effectively identify patients with AF, and the corresponding mechanism is discussed. The sensor can be carried and worn easily, without any impact on people's normal life. At the same time, it can be transmitted wirelessly and judged automatically without occupying medical resources. People can understand the results without medical experience. Based on the advantages of the sensor, 385 normal people/patient data were tested and analyzed. The diagnostic accuracy is 91%, especially the rate of missed detection is extremely low, so AFPW can play an important role in the physical examination for a large number of people. Therefore, AFPW is of great help in the diagnosis of AF patients. What's more, because the pulse wave signal contains a large amount of cardiovascular disease information, AFPW has the potential to be used in the diagnosis of other cardiovascular diseases, such as coronary heart disease, cardiomyopathy, heart failure, etc. AFPW may be used in intelligent medical treatment in the future.

## Acknowledgements

This study was supported by the National Natural Science Foundation of China (Nos. T2125003, 82202075, and 82102231), the Beijing Natural Science Foundation (Nos. JQ20038 and L212010), the National Postdoctoral Program for Innovative Talent (No. BX20220380), and the China Postdoctoral Science Foundation (No. 2022M710389). The authors thank everyone who contributed to this work.

**Electronic Supplementary Material:** Supplementary material (Figure S1. Comparison of signal output with and without enhancement layer; Figure S2. Relationship between force and electricity under low force conditions; Figure S3. Comparison of signals generated by different functional layers; Table S1. Comparison of SNR in similar research) is available in the online version of this article at https://doi.org/10.1007/s12274-023-5804-x.

## References

[1] Alonso, A.; Almuwaqqat, Z.; Chamberlain, A. Mortality in atrial fibrillation. Is it changing? *Trends Cardiovasc. Med.* **2021**, *31*, 469–473.

[2] Salih, M.; Abdel-Hafez, O.; Ibrahim, R.; Nair, R. Atrial fibrillation in the elderly population: Challenges and management considerations. *J. Arrhythmia* **2021**, *37*, 912–921.

[3] Song, J. S. The Chinese burden of atrial fibrillation review of atrial fibrillation studies in China. *Ann. Noninvasive Electrocardiol.* **2022**, *27*, e12957.

[4] Wang, Z. W.; Zhang, L. F.; Chen, Z.; Wang, X.; Li, S. N.; Dong, Y.; Zheng, C. Y.; Wang, J. L.; Kang, Y. T. A2528 the disease burden of atrial fibrillation in China: Data from a national cross-section survey. *J. Hypertens.* **2018**, *36*, E281.

[5] Bizhanov, K. A.; Abzaliyev, K. B.; Baimbetov, A. K.; Sarsenbayeva, A. B.; Lyan, E. Atrial fibrillation: Epidemiology, pathophysiology, and clinical complications (literature review). *J. Cardiovasc. Electrophysiol.* **2023**, *34*, 153–165.

[6] Collado, F. M. S.; Von Buchwald, C. M. L.; Anderson, C. K.; Madan, N.; Suradi, H. S.; Huang, H. D.; Jneid, H.; Kavinsky, C. J. Left atrial appendage occlusion for stroke prevention in nonvalvular atrial fibrillation. *J. Am. Heart Assoc.* **2021**, *10*, e022274.

[7] Wang, Y. C.; Xu, X. B.; Hajra, A.; Apple, S.; Kharawala, A.; Duarte, G.; Liaqat, W.; Fu, Y. W.; Li, W. J.; Chen, Y. Y. et al. Current advancement in diagnosing atrial fibrillation by utilizing wearable devices and artificial intelligence: A review study. *Diagnostics* **2022**, *12*, 689.

[8] Gunawardene, M. A.; Willems, S. Atrial fibrillation progression and the importance of early treatment for improving clinical outcomes. *Europace* **2022**, *24*, ii22–ii28.

[9] Tooley, J. E.; Perez, M. V. Role of digital health in detection and management of atrial fibrillation. *Heart* **2022**, *108*, 834–839.

[10] Duncker, D.; Ding, W. Y.; Etheridge, S.; Noseworth, P. A.; Veltmann, C.; Yao, X. X.; Bunch, T. J.; Gupta, D. Smart wearables for cardiac monitoring-real-world use beyond atrial fibrillation. *Sensors* **2021**, *21*, 2539.

[11] Sattar, Y.; Song, D.; Sarvepalli, D.; Zaidi, S. R.; Ullah, W.; Arshad, J.; Mir, T.; Zghouzi, M.; Elgendy, I. Y.; Qureshi, W. et al. Accuracy of pulsatile photoplethysmography applications or handheld devices vs. 12-lead ECG for atrial fibrillation screening: A systematic review and meta-analysis. *J. Interv. Card. Electrophysiol.* **2022**, *65*, 33–44.

[12] Kim, H. L.; Weber, T. Pulsatile hemodynamics and coronary artery disease. *Korean Circ. J.* **2021**, *51*, 881–898.

[13] Guo, C. X.; Jiang, Z. X.; He, H. Z.; Liao, Y. N.; Zhang, D. Wrist pulse signal acquisition and analysis for disease diagnosis: A review. *Comput. Biol. Med.* **2022**, *143*, 105312.

[14] Chen, G. R.; Au, C.; Chen, J. Textile triboelectric nanogenerators for wearable pulse wave monitoring. *Trends Biotechnol.* **2021**, *39*, 1078–1092.

[15] Meng, K. Y.; Xiao, X.; Wei, W. X.; Chen, G. R.; Nashalian, A.; Shen, S.; Xiao, X.; Chen, J. Wearable pressure sensors for pulse wave monitoring. *Adv. Mater.* **2022**, *34*, 2270158.

[16] Osawa, Y.; Hata, S.; Hori, M.; Dohi, T. Comparison of features by simultaneous measurement of blood pressure pulse wave and electrocardiogram. In *42nd Annual International Conference of the IEEE Engineering in Medicine & Biology Society (EMBC)*, Montreal, Canada, 2020, pp 4664–4667.

[17] Wegner, F. K.; Plagwitz, L.; Doldi, F.; Ellermann, C.; Willy, K.; Wolfes, J.; Sandmann, S.; Varghese, J.; Eckardt, L. Machine learning in the detection and management of atrial fibrillation. *Clin. Res. Cardiol.* **2022**, *111*, 1010–1017.

[18] Mainali, S.; Darsie, M. E.; Smetana, K. S. Machine learning in action: Stroke diagnosis and outcome prediction. *Front. Neurol.* **2021**, *12*, 734345.
[19] Chang, C. H.; Lin, C. H.; Lane, H. Y. Machine learning and novel biomarkers for the diagnosis of Alzheimer's disease. *Int. J. Mol. Sci.* **2021**, *22*, 2761.
[20] Wang, Y.; Zhu, L. P.; Du, C. F. Progress in piezoelectric nanogenerators based on PVDF composite films. *Micromachines* **2021**, *12*, 1278.
[21] Lee, C.; Park, H.; Lee, J. H. Recent structure development of poly(vinylidene fluoride)-based piezoelectric nanogenerator for self-powered sensor. *Actuators* **2020**, *9*, 57.
[22] Tan, P. C.; Xi, Y.; Chao, S. Y.; Jiang, D. J.; Liu, Z.; Fan, Y. B.; Li, Z. An artificial intelligence-enhanced blood pressure monitor wristband based on piezoelectric nanogenerator. *Biosensors* **2022**, *12*, 234.
[23] Cao, Y.; Yang, Y.; Qu, X. C.; Shi, B. J.; Xu, L. L.; Xue, J. T.; Wang, C.; Bai, Y.; Gai, Y. S.; Luo, D. et al. A self-powered triboelectric hybrid coder for human–machine interaction. *Small Methods* **2022**, *6*, 2101529.
[24] Kalimuldina, G.; Turdakyn, N.; Abay, I.; Medeubayev, A.; Nurpeissova, A.; Adair, D.; Bakenov, Z. A review of piezoelectric PVDF film by electrospinning and its applications. *Sensors* **2020**, *20*, 5214.
[25] Mirjalali, S.; Varposhti, A. M.; Abrishami, S.; Bagherzadeh, R.; Asadnia, M.; Huang, S. J.; Peng, S. H.; Wang, C. H.; Wu, S. Y. A review on wearable electrospun polymeric piezoelectric sensors and energy harvesters. *Macromol. Mater. Eng.* **2023**, *308*, 2200442.
[26] Arica, T. A.; Isık, T.; Guner, T.; Horzum, N.; Demir, M. M. Advances in electrospun fiber-based flexible nanogenerators for wearable applications. *Macromol. Mater. Eng.* **2021**, *306*, 2100143.
[27] Gai, Y. S.; Wang, E. G.; Liu, M. H.; Xie, L. R.; Bai, Y.; Yang, Y.; Xue, J. T.; Qu, X. C.; Xi, Y.; Li, L. L. et al. A self-powered wearable sensor for continuous wireless sweat monitoring. *Small Methods* **2022**, *6*, 2200653.
[28] Zhang, J.; Wang, Y. E.; Wei, Q. H.; Wang, Y. M.; Lei, M. J.; Li, M. Y.; Li, D. H.; Zhang, L. Y.; Wu, Y. Self-healing mechanism and conductivity of the hydrogel flexible sensors: A review. *Gels* **2021**, *7*, 216.
[29] Chao, S. Y.; Ouyang, H.; Jiang, D. J.; Fan, Y. B.; Li, Z. Triboelectric nanogenerator based on degradable materials. *EcoMat* **2021**, *3*, e12072.
[30] Wang, C.; Liu, Y.; Qu, X. C.; Shi, B. J.; Zheng, Q.; Lin, X. B.; Chao, S. Y.; Wang, C. Y.; Zhou, J.; Sun, Y. et al. Ultra-stretchable and fast self-healing ionic hydrogel in cryogenic environments for artificial nerve fiber. *Adv. Mater.* **2022**, *34*, 2105416.
[31] Liu, Y.; Wang, C.; Xue, J. T.; Huang, G. H.; Zheng, S.; Zhao, K.; Huang, J.; Wang, Y. Q.; Zhang, Y.; Yin, T. L. et al. Body temperature enhanced adhesive, antibacterial, and recyclable ionic hydrogel for epidermal electrophysiological monitoring. *Adv. Health. Mater.* **2022**, *11*, 2270092.
[32] Xu, J. P.; Tsai, Y. L.; Hsu, S. H. Design strategies of conductive hydrogel for biomedical applications. *Molecules* **2020**, *25*, 5296.
[33] Nele, V.; Wojciechowski, J. P.; Armstrong, J. P. K.; Stevens, M. M. Tailoring gelation mechanisms for advanced hydrogel applications. *Adv. Funct. Mater.* **2020**, *30*, 2002759.
[34] Mynard, J. P.; Kondiboyina, A.; Kowalski, R.; Cheung, M. M. H.; Smolich, J. J. Measurement, analysis, and interpretation of pressure/flow waves in blood vessels. *Front. Physiol.* **2020**, *11*, 1085.